Magnetoacoustic effects of electrical conductivity tensors for nonellipsoidal nonparabolic band structure*

Chhi-Chong Wu
College of Engineering, National Chiao Tung University, Hsinchu, Taiwan, China

Jensan Tsai
Institute of Nuclear Science, National Tsing Hua University, Hsinchu, Taiwan, China

(Received 24 July 1973)

Using time-independent perturbation theory, the energy eigenvalue equation for a free-electron gas in the presence of a dc magnetic field $\vec{B}$ is solved. The energy-band structure applied here is supposed to be the Cohen nonellipsoidal nonparabolic model. Then the longitudinal linear and nonlinear conductivity tensors are calculated by using the quantum-mechanical treatment which is valid in the high-frequency region. It is found that these conductivity tensors for ultrasound propagating parallel to the dc magnetic field depend upon the magnetic field and sound frequency. Some oscillations and discontinuities in these conductivity tensors are observed. This can be explained by the fact that the linear and nonlinear conductivity tensors have the logarithmic singularities of a purely quantum origin related to the degeneracy of the electron gas. We also present some numerical calculations of the absorption coefficient and change in sound velocity in bismuth. It is found that the absorption coefficient and change in sound velocity oscillate with the dc magnetic field and sound frequency when the ultrasound propagates parallel to the magnetic field.

I. INTRODUCTION

The constant energy surfaces in wave-vector space for real solids differ considerably from the simple spherical surfaces of the degenerate electron gas. The effects of the nonparabolicity of the conduction band in solids have been investigated by several authors.[1-8] There exist some materials in which the energy surfaces are much more complicated. Bismuth, for example, is a semimetal with highly anisotropic Fermi surfaces. Some recent works[9-13] have shown that the magnetic field dependence of some physical phenomena in a semimetal like bismuth can be explained by a two-band model for the energy bands. From theoretical calculations[14] and experimental results,[12,13] it has been pointed out that the energy band in the bismuth structure is the Cohen nonellipsoidal nonparabolic (NENP) model. The purpose of this paper is to present a detailed calculation of the longitudinal linear and nonlinear conductivity tensors by considering the spin-splitting effects for the NENP model as the energy-band structure of bismuth. These longitudinal components of the linear and nonlinear conductivity tensors play the dominant roles in determining the absorption coefficient and second-harmonic generation of ultrasonic waves in semiconductors and semimetals.[5,6,15,16] Therefore, we shall study these conductivity tensors for a system in which the Fermi surface is assumed to be the NENP model. Furthermore, we apply our results to discuss the effects of the NENP band structure on the ultrasonic absorption in bismuth.

In Sec. II the Schrödinger equation for an electron gas in a dc magnetic field $\vec{B}$ is solved by using time-independent perturbation theory. In Sec. III, the longitudinal linear and nonlinear conductivity tensors are obtained by using a quantum-mechanical treatment which is valid at high frequencies and in strong magnetic fields. Since this kind of treatment is valid for high frequencies such that $|\vec{q}|l \gg 1$, where $\vec{q}$ is the wave vector of the ultrasound and l is the electron mean free path, therefore the effect of collisions on the electrons is neglected. In Sec. IV some numerical calculations for a semimetal like bismuth are given. We also have a brief discussion about these numerical results.

II. SOLUTION OF ENERGY EIGENVALUE EQUATION

For convenience, we shall first consider the case without including the electron spin-splitting effect. In the NENP model, the relation between the energy and momentum of an electron gas in the absence of the dc magnetic field is assumed to be[14]

$$E\left(1+\frac{E}{E_g}\right)=\frac{p_x^2}{2m_1}+\frac{p_y^2}{2m_2}\left[1+\frac{E}{E_g}\left(1-\frac{m_2}{m_2'}\right)\right]+\frac{p_z^2}{2m_3}+\frac{p_y^4}{4m_2m_2'E_g}\,. \tag{1}$$

From the experimental results,[13,17] it has been indicated that the difference between m_2 and m_2' is quite small, i.e., $m_2 \approx m_2'$. Thus the term in the square brackets of Eq. (1) can be considered constant. For the sake of convenience, some parameters are defined as follows:

$$\alpha_1 = m/m_1\,,$$

$$\alpha_2 = (m/m_2)[1+(E/E_g)(1-m_2/m_2')] \approx m/m_2\,,$$

$$\alpha_3 = m/m_3 , \tag{2}$$

and

$$\alpha_4 = \frac{m}{2m_2 m_2' E_g} ,$$

where m is the mass of the free electron.

We now introduce a dc uniform magnetic field of induction $\vec{B}$ directed parallel to the z direction, then the vector potential in the Landau gauge can be expressed in the form $\vec{A}_0 = (0, Bx, 0)$. The energy eigenvalue equation can thus be written as

$$H_0(1 + H_0/E_g)\psi_{\vec{k}n} \equiv (1/2m)[\alpha_1 p_x^2 + \alpha_2(p_y - eBx/c)^2 + \alpha_3 p_z^2 + \alpha_4(p_y - eBx/c)^4]\psi_{\vec{k}n} = E_{\vec{k}n}(1 + E_{\vec{k}n}/E_g)\psi_{\vec{k}n} , \tag{3}$$

where $E_{\vec{k}n}$ is the true energy of the system defined by $H_0\psi_{\vec{k}n} = E_{\vec{k}n}\psi_{\vec{k}n}$, and E_g is the energy gap between the conduction and valence bands. Then, by considering $H' = (\alpha_4/2m)(p_y - eBx/c)^4$ as a perturbation term, the eigenfunctions and eigenvalues up to first order for Eq. (3) are given by

$$\psi_{\vec{k}n}(\vec{r}) = e^{ik_y y + ik_z z}\{\phi_n(x - x_0) + (\delta/16\hbar\omega_c)[n(n-1)(n-2)(n-3)]^{1/2}\phi_{n-4}(x - x_0) + (\delta/4\hbar\omega_c)[n(n-1)]^{1/2}(2n-1)\phi_{n-2}(x - x_0) - (\delta/4\hbar\omega_c)[(n+1)(n+2)]^{1/2}(2n+3)\phi_{n+2}(x - x_0) - (\delta/16\hbar\omega_c)[(n+1)(n+2)(n+3)(n+4)]^{1/2}\phi_{n+4}(x - x_0)\} \tag{4}$$

and

$$E_{\vec{k}n} = -\tfrac{1}{2}E_g(1 - \{1 + (4/E_g)[(n + \tfrac{1}{2})\hbar\omega_c + \hbar^2 k_z^2/2m^* + \tfrac{3}{2}\delta(n^2 + n + \tfrac{1}{2})]\}^{1/2}) , \tag{5}$$

where $\omega_c = (|e|B/mc)(\alpha_1\alpha_2)^{1/2}$, $\delta = (\alpha_1\alpha_4/\alpha_2) \times (e^2B^2\hbar^2/2mc^2)$, $x_0 = \hbar c k_y/eB$, $m^* = m/\alpha_3$, and $\phi_n(x)$ is the harmonic-oscillator wave function.

If the electron spin-splitting effect is taken into account, the eigenfunctions become

$$\psi_{\vec{k}ns}(\vec{r}) = \begin{pmatrix} \frac{1+s}{2} \\ \frac{1-s}{2} \end{pmatrix} \psi_{\vec{k}n}(\vec{r}) , \tag{6}$$

where $\psi_{\vec{k}n}(\vec{r})$ are given by Eq. (4) and $s = \pm 1$. Similarly, the eigenvalues of the system are given by

$$E_{\vec{k}ns} = -\tfrac{1}{2}E_g(1 - \{1 + (4/E_g)[(n + \tfrac{1}{2})\hbar\omega_c + \tfrac{1}{2}s\hbar\omega_s + \hbar^2 k_z^2/2m^* + (3\delta/2)(n^2 + n + \tfrac{1}{2})]\}^{1/2}) , \tag{7}$$

where ω_s is defined by $\omega_s = |e|B/m_s c$, and m_s is the spin effective mass which has a relation with the spin-splitting factor g such that $m_s/m = 2/g$. For bismuth, the spin effective mass is equal to the cyclotron mass,[10,18,19] i.e., $m_s = m/(\alpha_1\alpha_2)^{1/2}$. Therefore $\omega_s = \omega_c$ in pure bismuth.

III. LONGITUDINAL LINEAR AND NONLINEAR CONDUCTIVITY TENSORS

The calculation of the longitudinal linear and nonlinear conductivity tensors follows the same procedure as that described in an earlier paper.[16] The interaction of the conduction electrons with the ultrasound can be taken into account via the vector potential $\vec{A}_1 = \vec{A}_{10}\exp(i\vec{q}\cdot\vec{r} - i\omega t)$ which arises from the self-consistent field accompanying the ultrasonic wave. It is also assumed that the deformation-potential coupling dominates the interaction. To second order in $\vec{A}_1$ the Hamiltonian for an electron in the presence of the dc magnetic field $\vec{B}$ and self-consistent field is

$$H = H_0 + H_1 + H_2 . \tag{8}$$

Here, H_0 is the Hamiltonian of an electron in the dc magnetic field $\vec{B}$ and is given by the relation

$$F(p_x, p_y, p_z) \equiv H_0(1 + H_0/E_g) = (1/2m)[\alpha_1 p_x^2 + \alpha_2(p_y - eBx/c)^2 + \alpha_3 p_z^2 + \alpha_4(p_y - eBx/c)^4] + i\vec{q}\cdot\overleftrightarrow{C}\cdot\vec{\xi} , \tag{9}$$

where $\overleftrightarrow{C}$ is the deformation-potential tensor for one type of carrier being dominant, and $\vec{\xi} = \vec{\xi}_0\exp(i\vec{q}\cdot\vec{r} - i\omega t)$ is the displacement of atoms in solids. The first-order Hamiltonian due to the self-consistent field, H_1, is given by

$$H_1 = -\left(\frac{e}{2c}\right)\left(1 + \frac{2H_0}{E_g}\right)^{-1}\left(A_{1i}\frac{\partial F}{\partial p_i} + \frac{\partial F}{\partial p_i}A_{1i}\right) . \tag{10}$$

The second-order Hamiltonian due to the self-consistent field, H_2, is given by

$$H_2 = \left(\frac{e^2}{2c^2}\right)\left(1 + \frac{2H_0}{E_g}\right)^{-1}\left[\frac{\partial^2 F}{\partial p_i \partial p_j}A_{1i}A_{1j} - \frac{1}{2E_g}\left(1 + \frac{2H_0}{E_g}\right)^{-2} \times \left(A_{1i}\frac{\partial F}{\partial p_i} + \frac{\partial F}{\partial p_i}A_{1i}\right)\left(A_{1j}\frac{\partial F}{\partial p_j} + \frac{\partial F}{\partial p_j}A_{1j}\right)\right] . \tag{11}$$

Using the gauge where the scalar potential is zero, the relation between the self-consistent field $\vec{E}$ and the vector potential $\vec{A}_1$ is found to be

$$\vec{E} = (i\omega/c)\vec{A}_1 . \tag{12}$$

Following the same method of quantum treatment

as our previous papers,[5,6,16] we obtain the current density expressed in the form

$$J_i = \sigma_{ij}\left[E_j - \frac{\partial}{\partial x_j}\left(\frac{C_{lm}}{e}S_{lm}\right)\right] + \tau_{ijk}\left[E_j - \frac{\partial}{\partial x_j}\left(\frac{C_{lm}}{e}S_{lm}\right)\right] \times \left[E_k - \frac{\partial}{\partial x_k}\left(\frac{C_{np}}{e}S_{np}\right)\right], \quad (13)$$

where C_{lm} is the deformation potential tensor and S_{ij} is the strain tensor. From Eq. (13), one can find the linear and nonlinear conductivity tensors as functions of the ultrasonic wave vector $\vec{q}$ and frequency ω. It has been shown that the longitudinal magnetoacoustic phenomena and acoustic flux in the second harmonic depend upon the longitudinal components of the linear and nonlinear conductivity tensors σ_{zz} and τ_{zzz}.[5,15,16] Therefore, in our present case, the only components of the conductivity tensors of interest are σ_{zz} and τ_{zzz}. It can readily be found that

$$\sigma_{zz}(\vec{q},\omega) = \frac{\omega_p^2}{4\pi i\omega n_0}\left[\alpha_3 \sum_{\vec{k}ns} f_{\vec{k}ns}\theta_{\vec{k}ns} - (\alpha_3^2\hbar^2/4m)\sum_{\vec{k}nn's} \frac{(f_{\vec{k}ns} - f_{\vec{k}+\vec{q},n's})\theta_{\vec{k}ns}\theta_{\vec{k}+\vec{q},n's}}{E_{\vec{k}+\vec{q},n's} - E_{\vec{k}ns} - \hbar\omega}(2k_z + q_z)^2 N_{n'n}(q_x,q_y,0)N_{n'n}(-q_x,q_y,0)\right] \quad (14)$$

and

$$\tau_{zzz}(\vec{q},\omega) = -\frac{3\omega_p^2 e q_z \hbar\alpha_3^2}{4\pi m\omega^2 E_g n_0}\sum_{\vec{k}ns} f_{\vec{k}ns}\theta_{\vec{k}ns}^3 - \frac{\omega_p^2 e\hbar\alpha_3^2}{8\pi\omega^2 n_0 m}\left[\sum_{\vec{k}nn's} \frac{(f_{\vec{k}ns} - f_{\vec{k}+\vec{q},n's})\theta_{\vec{k}ns}\theta_{\vec{k}+\vec{q},n's}}{E_{\vec{k}+\vec{q},n's} - E_{\vec{k}ns} - \hbar\omega}(2k_z + q_z)N_{n'n}(q_x,q_y,0)N_{n'n}(-q_x,q_y,0)\right.$$

$$+ \sum_{\vec{k}nn's} \frac{(f_{\vec{k}ns} - f_{\vec{k}+2\vec{q},n's})\theta_{\vec{k}ns}\theta_{\vec{k}+2\vec{q},n's}}{E_{\vec{k}+2\vec{q},n's} - E_{\vec{k}ns} - 2\hbar\omega}(k_z + q_z)N_{n'n}(2q_x,2q_y,0)N_{n'n}(-2q_x,2q_y,0)$$

$$- (\hbar^2\alpha_3/2m)\sum_{\vec{k}nn'n''s} F(\vec{k},\vec{k}+2\vec{q},\vec{k}+\vec{q};n,n',n'';s)\theta_{\vec{k}ns}\theta_{\vec{k}+2\vec{q},n's}\theta_{\vec{k}+\vec{q},n''s}$$

$$\left.\times(2k_z + q_z)(k_z + q_z)(2k_z + 3q_z)N_{n'n''}(q_x,q_y,0)N_{n''n}(q_x,q_y,0)N_{n'n}(-2q_x,2q_y,0)\right], \quad (15)$$

where $\omega_p = (4\pi n_0 e^2/m)^{1/2}$ is the plasma frequency of the free electron with the mass m and $\theta_{\vec{k}ns}$ is given by

$$\theta_{\vec{k}ns} = (1 + 2E_{\vec{k}ns}/E_g)^{-1}. \quad (16)$$

The functions $N_{n'n}(q_x,q_y,x_0)$ and $F(\vec{k},\vec{k}+2\vec{q},\vec{k}+\vec{q};n,n',n'';s)$ are defined as follows:

$$N_{n'n}(q_x,q_y,x_0) = \int_{-\infty}^{+\infty}\phi_{n'}(x - x_0')\,e^{iq_x x}\phi_n(x - x_0)\,dx, \quad (17)$$

where $x_0 = ck_y\hbar/eB$, and $x_0' = cK_y\hbar/eB$ for $K_y = k_y + q_y$ or $k_y + 2q_y$;

$$F(\vec{k},\vec{k}+2\vec{q},\vec{k}+\vec{q};n,n',n'';s) = [f_{\vec{k}+2\vec{q},n's}(E_{\vec{k}+\vec{q},n''s} - E_{\vec{k}ns} - \hbar\omega) - f_{\vec{k}+\vec{q},n''s}(E_{\vec{k}+2\vec{q},n's} - E_{\vec{k}ns} - 2\hbar\omega) + f_{\vec{k}ns}(E_{\vec{k}+2\vec{q},n's} - E_{\vec{k}+\vec{q},n''s} - \hbar\omega)]$$

$$\times[(E_{\vec{k}+2\vec{q},n's} - E_{\vec{k}ns} - 2\hbar\omega)(E_{\vec{k}+2\vec{q},n's} - E_{\vec{k}+\vec{q},n''s} - \hbar\omega)(E_{\vec{k}+\vec{q},n''s} - E_{\vec{k}ns} - \hbar\omega)]^{-1}. \quad (18)$$

IV. NUMERICAL RESULTS AND DISCUSSION

In our present case we are interested in an acoustic wave propagating parallel to the dc magnetic field, i.e., $q_x = q_y = 0$, and $\vec{q} = q\hat{z}$. The distribution function of electrons in a semimetal like bismuth is represented by the Fermi-Dirac statistics. The interesting temperature is assumed to be very near absolute zero. Consequently, the eigenvalues of the system in Eq. (7) can be expanded as

$$E_{\vec{k}ns} \cong -\tfrac{1}{2}E_g + \tfrac{1}{2}E_g a_{ns} + \hbar^2 k_z^2/2m^* a_{ns}, \quad (19)$$

where

$$a_{ns} = \{1 + (4/E_g)[(n + \tfrac{1}{2})\hbar\omega_c + \tfrac{1}{2}s\hbar\omega_s + \tfrac{3}{2}\delta(n^2 + n + \tfrac{1}{2})]\}^{1/2}. \quad (20)$$

Using Eqs. (6) and (19) in (14) and (15), we obtain

$$\sigma_{zz}(\vec{q},\omega) = i(\omega_p^*)^2\left(8\sqrt{2}\,\pi\omega\sum_{n,s}(\Delta E_{ns})^{1/2}\right)^{-1}\left(-(E_g)^{1/2}\sum_{n,s}\tan^{-1}\left(\frac{2\sqrt{2}\,a_{ns}(\Delta E_{ns}E_g)^{1/2}}{a_{ns}^2 E_g - 2(\Delta E_{ns})}\right)\right.$$

$$+\frac{(m^*)^{3/2}E_g^2}{4q\hbar^3}\sum_{n,s}a_{ns}^3\left[\left(\frac{q^2}{4}+\frac{\omega^2(m^*)^2a_{ns}^2}{q^2\hbar^2}+\frac{m^*a_{ns}^2E_g}{\hbar^2}\right)^2-\frac{\omega^2(m^*)^2a_{ns}^2}{\hbar^2}\right]^{-1}$$

$$\times\left\{\frac{4\omega^2(m^*)^2a_{ns}^2}{q^2\hbar^2}\left[\ln\left(\frac{(\Delta E_{ns})^{1/2}+q\hbar/2\sqrt{2}\,(m^*)^{1/2}-\omega(m^*)^{1/2}a_{ns}/\sqrt{2}\,q}{-(\Delta E_{ns})^{1/2}+q\hbar/2\sqrt{2}\,(m^*)^{1/2}-\omega(m^*)^{1/2}a_{ns}/\sqrt{2}\,q}\right)\right.\right.$$

$$-\ln\left(\frac{(\Delta E_{ns})^{1/2}-q\hbar/2\sqrt{2}\,(m^*)^{1/2}-\omega(m^*)^{1/2}a_{ns}/\sqrt{2}\,q}{-(\Delta E_{ns})^{1/2}-q\hbar/2\sqrt{2}\,(m^*)^{1/2}-\omega(m^*)^{1/2}a_{ns}/\sqrt{2}\,q}\right)$$

$$\left.-\tfrac{1}{2}\ln\left(\frac{[(\Delta E_{ns})^{1/2}+q\hbar/\sqrt{2}\,(m^*)^{1/2}]^2+\frac{1}{2}a_{ns}^2E_g}{[-(\Delta E_{ns})^{1/2}+q\hbar/\sqrt{2}\,(m^*)^{1/2}]^2+\frac{1}{2}a_{ns}^2E_g}\right)\right]+\frac{\hbar}{(m^*E_g)^{1/2}a_{ns}}\left[\frac{q^3}{4}+\frac{2m^*a_{ns}^2qE_g}{\hbar^2}-\frac{\omega^2(m^*)^2a_{ns}^2}{q\hbar^2}\right.$$

$$\left.\left.+\frac{4(m^*)^2a_{ns}^4E_g^2}{q\hbar^4}+\frac{4\omega^2(m^*)^3a_{ns}^4E_g}{q^3\hbar^4}\right]\left[\tan^{-1}\left(\frac{2\sqrt{2}\,a_{ns}(\Delta E_{ns}E_g)^{1/2}}{a_{ns}^2E_g-2(\Delta E_{ns})}\right)-\tan^{-1}\left(\frac{2\sqrt{2}\,a_{ns}(\Delta E_{ns}E_g)^{1/2}}{a_{ns}^2-2(\Delta E_{ns})+q^2\hbar^2/m^*}\right)\right]\right\}\Bigg) \tag{21}$$

and

$$\tau_{zzz}(\vec{q},\omega)=-\frac{3(\omega_p^*)^2eq\hbar}{32\pi m^*\omega^2E_g\sum_{n,s}(\Delta E_{ns})^{1/2}}\sum_{n,s}\frac{(\Delta E_{ns})^{1/2}(5+6\Delta E_{ns}/a_{ns}^2E_g)}{a_{ns}^3(1+2\Delta E_{ns}/a_{ns}^2E_g)^2}$$

$$-\frac{(\omega_p^*)^2e\hbar}{16\sqrt{2}\,\pi\omega^2m^*\sum_{n,s}(\Delta E_{ns})^{1/2}}\sum_{n,s}\left[A_{ns}(\vec{q},\omega)\tan^{-1}\left(\frac{2\sqrt{2}\,a_{ns}(\Delta E_{ns}E_g)^{1/2}}{a_{ns}^2E_g-2(\Delta E_{ns})}\right)\right.$$

$$+B_{ns}(\vec{q},\omega)\tan^{-1}\left(\frac{2\sqrt{2}\,a_{ns}(\Delta E_{ns}E_g)^{1/2}}{a_{ns}^2E_g-2(\Delta E_{ns})+q^2\hbar^2/m^*}\right)+C_{ns}(\vec{q},\omega)\tan^{-1}\left(\frac{2\sqrt{2}\,a_{ns}(\Delta E_{ns}E_g)^{1/2}}{a_{ns}^2E_g-2(\Delta E_{ns})+4q^2\hbar^2/m^*}\right)$$

$$+D_{ns}(\vec{q},\omega)\ln\left(\frac{(\Delta E_{ns})^{1/2}+q\hbar/2\sqrt{2}\,(m^*)^{1/2}-\omega(m^*)^{1/2}a_{ns}/\sqrt{2}\,q}{-(\Delta E_{ns})^{1/2}+q\hbar/2\sqrt{2}\,(m^*)^{1/2}-\omega(m^*)^{1/2}a_{ns}/\sqrt{2}\,q}\right)$$

$$+E_{ns}(\vec{q},\omega)\ln\left(\frac{(\Delta E_{ns})^{1/2}-q\hbar/2\sqrt{2}\,(m^*)^{1/2}-\omega(m^*)^{1/2}a_{ns}/\sqrt{2}\,q}{-(\Delta E_{ns})^{1/2}-q\hbar/2\sqrt{2}\,(m^*)^{1/2}-\omega(m^*)^{1/2}a_{ns}/\sqrt{2}\,q}\right)$$

$$+F_{ns}(\vec{q},\omega)\ln\left(\frac{(\Delta E_{ns})^{1/2}+q\hbar/\sqrt{2}\,(m^*)^{1/2}-\omega(m^*)^{1/2}a_{ns}/\sqrt{2}\,q}{-(\Delta E_{ns})^{1/2}+q\hbar/\sqrt{2}\,(m^*)^{1/2}-\omega(m^*)^{1/2}a_{ns}/\sqrt{2}\,q}\right)$$

$$+G_{ns}(\vec{q},\omega)\ln\left(\frac{(\Delta E_{ns})^{1/2}-q\hbar/\sqrt{2}\,(m^*)^{1/2}-\omega(m^*)^{1/2}a_{ns}/\sqrt{2}\,q}{-(\Delta E_{ns})^{1/2}-q\hbar/\sqrt{2}\,(m^*)^{1/2}-\omega(m^*)^{1/2}a_{ns}/\sqrt{2}\,q}\right)$$

$$+H_{ns}(\vec{q},\omega)\ln\left(\frac{[(\Delta E_{ns})^{1/2}+q\hbar/\sqrt{2}\,(m^*)^{1/2}]^2+\frac{1}{2}a_{ns}E_g}{[-(\Delta E_{ns})^{1/2}+q\hbar/\sqrt{2}\,(m^*)^{1/2}]^2+\frac{1}{2}a_{ns}E_g}\right)$$

$$+I_{ns}(\vec{q},\omega)\ln\left(\frac{[(\Delta E_{ns})^{1/2}+\sqrt{2}\,q\hbar/(m^*)^{1/2}]^2+\frac{1}{2}a_{ns}E_g}{[-(\Delta E_{ns})^{1/2}+\sqrt{2}\,q\hbar/(m^*)^{1/2}]^2+\frac{1}{2}a_{ns}E_g}\right)$$

$$\left.-\left(\frac{4\sqrt{2}\,(m^*)^5a_{ns}^5E_g^3(\Delta E_{ns})^{3/2}}{3q^2\hbar^{10}}\right)J_{ns}(\vec{q},\omega)-\left(\frac{(m^*)^4a_{ns}^5E_g^3(\Delta E_{ns})^{1/2}}{\sqrt{2}\,q^2\hbar^8}\right)K_{ns}(\vec{q},\omega)\right], \tag{22}$$

where $\omega_p^*=(4\pi n_0e^2/m^*)^{1/2}$ is the plasma frequency of the electron with the effective mass m^*, and $\Delta E_{ns}=E_F(1+E_F/E_g)-(n+\frac{1}{2})\hbar\omega_c-\frac{1}{2}s\hbar\omega_s-\frac{3}{2}\delta(n^2+n+\frac{1}{2})$. The functions $A_{ns}(\vec{q},\omega)$, $B_{ns}(\vec{q},\omega)$, $C_{ns}(\vec{q},\omega)$, $D_{ns}(\vec{q},\omega)$, $E_{ns}(\vec{q},\omega)$, $F_{ns}(\vec{q},\omega)$, $G_{ns}(\vec{q},\omega)$, $H_{ns}(\vec{q},\omega)$, $I_{ns}(\vec{q},\omega)$, $J_{ns}(\vec{q},\omega)$, and $K_{ns}(\vec{q},\omega)$ are given in the Appendix.

As a numerical example for bismuth, the relevant parameters are[20] $n_0=2.75\times10^{17}$ cm^{-3}, $\alpha_1=172$, $\alpha_2=0.8$, $\alpha_3=88.5$, $E_g=0.0153$ eV, $E_F=0.0276$ eV, and $v_s=10^5$ cm/sec. The numerical results for the conductivity tensors σ_{zz} and τ_{zzz} as functions of sound frequency ω are shown in Figs. 1 and 2. It can be seen that both $\mathrm{Re}[\sigma_{zz}]$ and $\mathrm{Im}[-\sigma_{zz}]$ decrease with increasing the sound frequency. We can also see that some oscillations and discontinuities appear in the microwave region. In Fig. 2, it is shown that the absolute values of $\mathrm{Re}[\tau_{zzz}]$ is much larger than those of $\mathrm{Im}[\tau_{zzz}]$. Moreover, there is a minimum point of $\mathrm{Re}[\tau_{zzz}]$ in the neighborhood of $\omega=4\times10^{10}$ rad/sec. It has been shown that the acoustic flux in the second harmonic is proportional to $|\tau_{zzz}|^2$.[16]

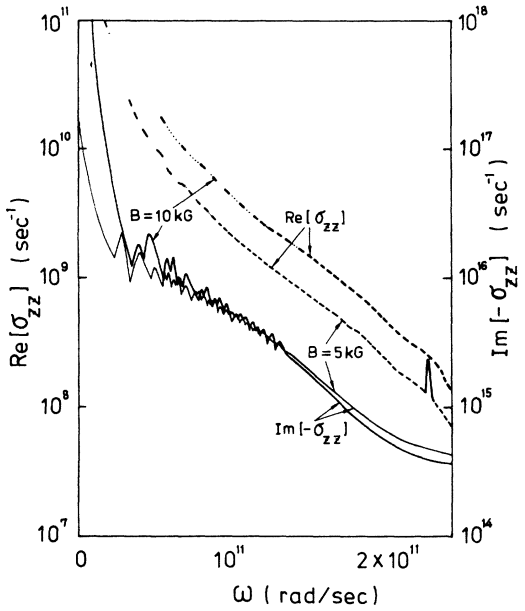

FIG. 1. Real part and imaginary part of the longitudinal linear conductivity tensor σ_{zz} as a function of sound frequency ω for nonellipsoidal nonparabolic band structure in bismuth.

Consequently, the real part of τ_{zzz} will dominate the second-harmonic generation and the acoustic flux in the second harmonic will have a minimum value in the neighborhood of $\omega = 4\times10^{10}$ rad/sec in bismuth. The imaginary part of τ_{zzz} oscillates with the sound frequency in the microwave region. As the magnetic field and sound frequency increase, these oscillations will be diminished and washed out in the region of very strong magnetic fields and high frequencies. The magnetic field dependence of the linear and nonlinear conductivity tensors is shown in Figs. 3 and 4. It can be seen that the real part of σ_{zz} increases with the magnetic field. However, these curves are not continuous. The imaginary part of σ_{zz} oscillates considerably with the magnetic field in the region of strong magnetic fields. These oscillations will also be washed out when the sound frequency increases above the microwave region. Therefore the effect of screening will be broken down in high frequencies. It is also shown that the imaginary part of τ_{zzz} oscillates with the magnetic field. However, the real part of τ_{zzz} is almost independent of the magnetic field.

It has been assumed that the interaction between the conduction electrons and the ultrasound in semimetals is via deformation potential coupling. Then the relation between the absorption coefficient and the ac conductivity tensor $\sigma_{zz}(\tilde{q}, \omega)$ for one type of carrier being dominant in the presence of a magnetic field is given by[21]

$$\alpha_{\parallel} = -\frac{\epsilon}{4\pi d v_s^2}\left(\frac{\omega}{v_s}\right)^3\left(\frac{C}{e}\right)^2 \mathrm{Im}\left(1-\frac{4\pi\sigma_{zz}}{i\omega\epsilon}\right)^{-1}, \quad (23)$$

where d is the density of the material, ϵ is the static dielectric constant, v_s is the sound velocity,

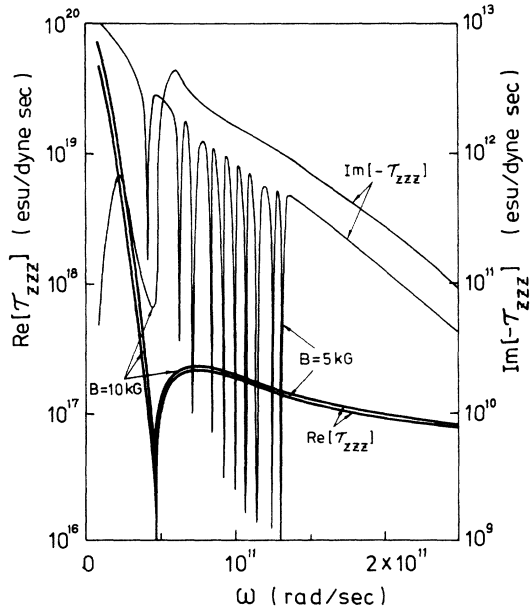

FIG. 2. Real part and imaginary part of the longitudinal nonlinear conductivity tensor τ_{zzz} as a function of sound frequency ω for nonellipsoidal nonparabolic band structure in bismuth.

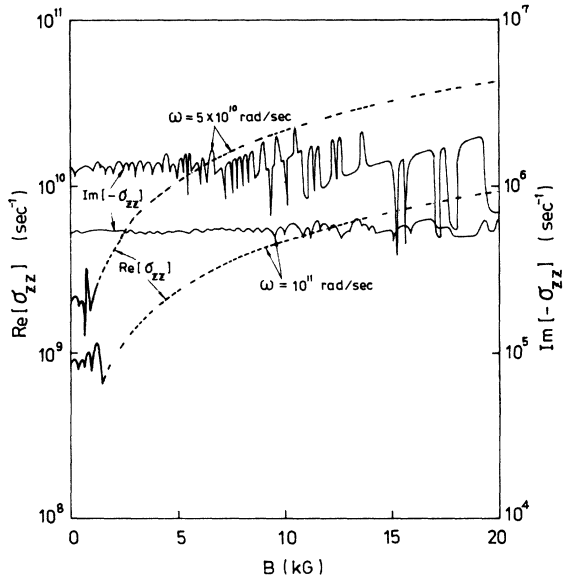

FIG. 3. Real part and imaginary part of the longitudinal linear conductivity tensor σ_{zz} as a function of dc magnetic field B for nonellipsoidal nonparabolic band structure in bismuth.

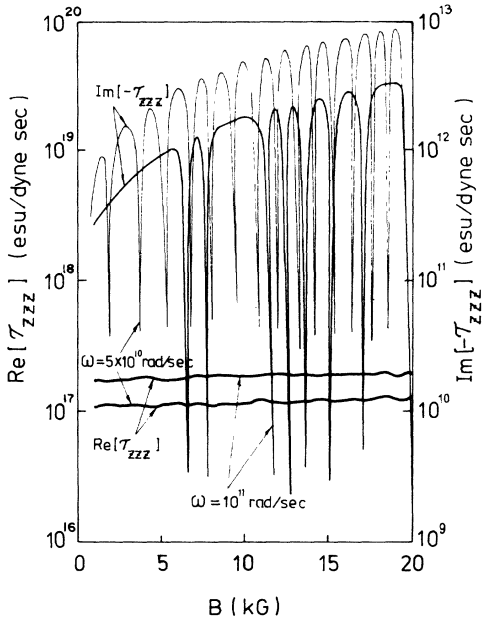

FIG. 4. Real part and imaginary part of the longitudinal nonlinear conductivity tensor τ_{zzz} as a function of dc magnetic field B for nonellipsoidal nonparabolic band structure in bismuth.

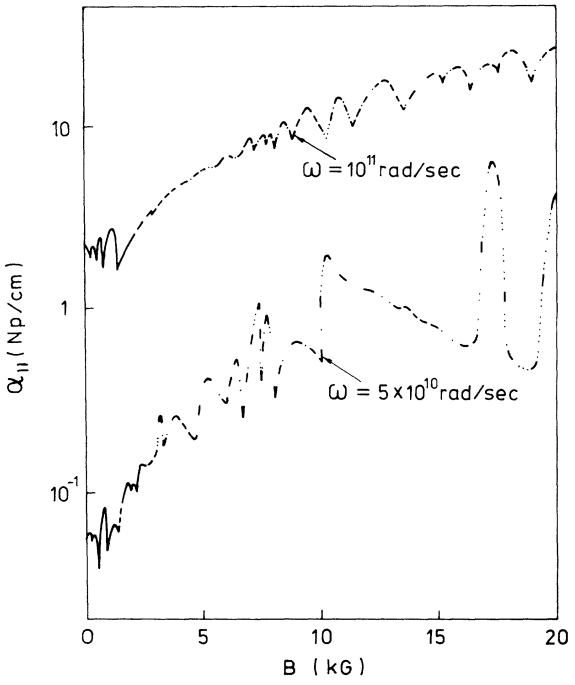

FIG. 5. Absorption coefficient $\alpha_{\parallel}$ as a function of dc magnetic field B for NENP model in bismuth. Broken lines indicate that somewhere the absorption coefficient $\alpha_{\parallel}$ will vanish.

and C is the deformation potential. Since the ratio of the sound velocity to the velocity of light is about 10^{-5}, therefore the absorption coefficient due to the longitudinal-induced field is much larger than that due to the transverse-induced field.[15] This means that the longitudinal component of the conductivity tensor plays the dominant role in determining the dispersion and absorption of ultrasounds in the presence of the longitudinal dc magnetic field in solids. The change in the sound velocity due to the interaction between the conduction electrons and the ultrasound is also related to the ac conductivity tensor $\sigma_{zz}(\vec{q}, \omega)$:

$$\frac{\Delta v_s}{v_s} = \frac{\epsilon}{8\pi d v_s^2}\left(\frac{\omega}{v_s}\right)^2\left(\frac{C}{e}\right)^2 \mathrm{Re}\left(1 - \frac{4\pi\sigma_{zz}}{i\omega\epsilon}\right)^{-1} . \qquad (24)$$

The numerical values of C, ϵ, and d for bismuth may take[22] $C = 10$ eV, $\epsilon = 10$, and $d = 9.8$ g/cm^3. The results for the absorption coefficient and the change in sound velocity as functions of magnetic field are shown in Figs. 5 and 6. It is shown that both the absorption coefficient and change in sound velocity oscillate with the magnetic field and some discontinuities can be observed. These oscillations and discontinuities appear considerably more by increasing the magnetic field. However, these oscillations will be diminished with increasing the sound frequency. In Fig. 5, we can see that the absorption coefficient increases slowly with the magnetic field even though it will vanish in some regions of the magnetic field. In Fig. 6, it is shown that the change in sound velocity oscillates with the magnetic field, but does not change its order of magnitude. This result for the change in sound velocity being oscillatory with magnetic field is quite different from our previous result in the case of a degenerate semiconductor like n-type InSb,[23] in which the change in sound velocity was

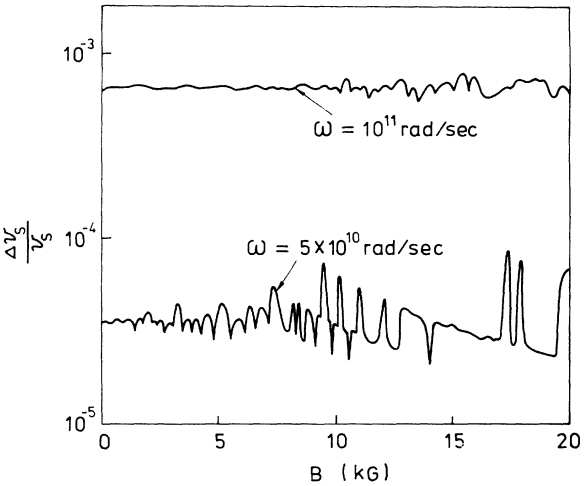

FIG. 6. Change in sound velocity $\Delta v_s/v_s$ as a function of dc magnetic field B for NENP model in bismuth.

shown to be independent of the magnetic field. We have also plotted the absorption coefficient and change in sound velocity as functions of sound frequency as shown in Figs. 7 and 8. It shows that the absorption coefficient increases with the sound frequency. The change in sound velocity increases very rapidly with the sound frequency and some oscillations can be observed in the region of strong magnetic fields. However, when the sound frequency is higher than $\omega = 2\times10^{11}$ rad/sec, the oscillations will be washed out due to the breakdown of screening in solids.

From the results of our calculations presented here, it is shown that both the absorption coefficient and change in sound velocity of the longitudinal ultrasound travelling parallel to the dc magnetic field exhibit oscillations as functions of the magnetic field and sound frequency. Since we are interested in the frequencies in the microwave region such that $|\vec{q}|l \gg 1$, therefore these oscillations can be interpreted as the so-called "giant quantum oscillations."[24-26] These oscillations occur in a degenerate electron gas in the case when the electron level is near the Fermi surface and the sound wave vector $\vec{q}$ has a component along the dc magnetic field. However, in our previous works,[23] it was found that the giant quantum oscillations occur only in the absorption coefficient as functions of the sound frequency and magnetic field. In the present case, owing to the nonlinear effect of the energy surface of NENP model in bismuth, the change in sound velocity will depend upon the magnetic field and sound frequency. Furthermore, some oscillations and discontinuities in the change of sound velocity can be observed. The nonlinear factor δ, which is proportional to the square of the dc magnetic field, will contribute to the energy level of electrons in bismuth. And this factor is included in the parameter a_{ns}. Thus the parameter a_{ns} is a function of magnetic field due to the contribution of these parameters ω_c, ω_s, and δ. This effect of NENP model in the band structure of bismuth is to introduce an energy, and therefore, a magnetic-field-dependent effective mass for the electrons. This effective mass for electrons in an energy level of quantum number n and spin quantum number s is $m^* a_{ns}$. Consequently the effective mass of electrons defined by $m^* a_{ns}$ depends strongly upon the magnetic field.

It can also be found that some discontinuities in the absorption coefficient are shown to vanish owing to the real part of the longitudinal conductivity tensor being zero. This means that no energy can be transferred between the conduction electrons and ultrasound in bismuth in some regions of magnetic field and sound frequency. It was found that the real part of the conductivity σ_{zz} in bismuth is not continuous.[27] This can be explained by the fact that the conductivity σ_{zz} has the logarithmic singu-

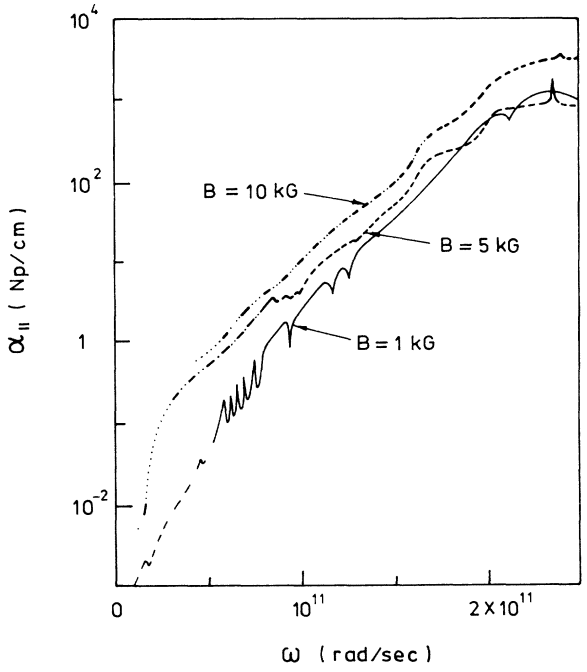

FIG. 7. Absorption coefficient $\alpha_{\parallel}$ as a function of sound frequency ω for NENP model in bismuth. Broken lines indicate that somewhere the absorption coefficient $\alpha_{\parallel}$ will vanish.

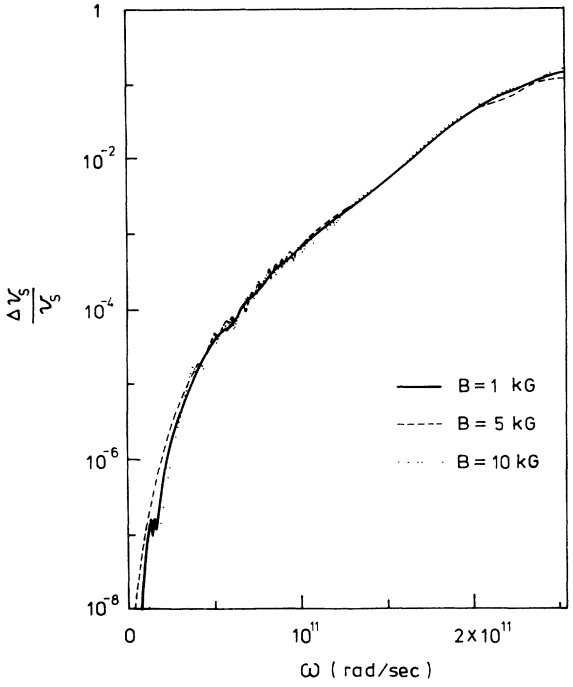

FIG. 8. Change in sound velocity $\Delta v_s/v_s$ as a function of sound frequency ω for NENP model in bismuth.

larities of a purely quantum origin related to the degeneracy of the electron gas.[26,28] When the sound frequency increases, the screening effect will be diminished. At high frequencies there is no longer any screening of the electron-phonon interaction in solids, therefore the change in sound velocity does not depend upon the longitudinal conductivity.[6] Since bismuth is a semimetal with highly anisotropic Fermi surfaces, the oscillations and discontinuities in the attenuation of ultrasound in bismuth depend upon the magnetic field owing to the nonellipsoidal nonparabolicity of the energy levels.

ACKNOWLEDGMENT

One of us (C.-C.W.) would like to express his gratitude to Professor Harold N. Spector for many valuable discussions.

APPENDIX

Functions $A_{ns}(\vec{q},\omega)$, $B_{ns}(\vec{q},\omega)$, $C_{ns}(\vec{q},\omega)$, $D_{ns}(\vec{q},\omega)$, $E_{ns}(\vec{q},\omega)$, $F_{ns}(\vec{q},\omega)$, $G_{ns}(\vec{q},\omega)$, $H_{ns}(\vec{q},\omega)$, $I_{ns}(\vec{q},\omega)$, $J_{ns}(\vec{q},\omega)$, and $K_{ns}(\vec{q},\omega)$ in Eq. (22) are given as follows:

$$A_{ns}(\vec{q},\omega)=\frac{9q}{4a_{ns}^2(E_g)^{1/2}}+(m^*)^2a_{ns}^2E_g^{3/2}L_1(q^2\hbar^2+4m^*a_{ns}^2E_g)^{-1}\left(\frac{m^*a_{ns}\omega q}{2\hbar^3}-\frac{2m^{*3}a_{ns}^3\omega^3}{q^3\hbar^5}-\frac{8m^{*4}a_{ns}^5E_g\omega^3}{q^5\hbar^7}-\frac{8m^{*3}a_{ns}^5E_g\omega}{q^3\hbar^7}\right)$$
$$+m^{*2}a_{ns}^2E_g^{3/2}L_2(q^2\hbar^2+m^*a_{ns}^2E_g)^{-1}\left(\frac{m^*a_{ns}\omega q}{4\hbar^3}-\frac{m^{*3}a_{ns}^3\omega^3}{4q^3\hbar^5}-\frac{m^{*4}a_{ns}^5E_g\omega^3}{4q^5\hbar^7}-\frac{m^{*3}a_{ns}^5E_g^2\omega}{4q^3\hbar^7}\right)$$
$$-\frac{m^{*3}a_{ns}^4E_g^{5/2}}{4q^2\hbar^{10}}(-11m^*a_{ns}^2q^2\hbar^2E_gP_1+4m^{*2}a_{ns}^4E_gP_1+12m^*a_{ns}^2q\hbar^2E_gP_2-3q^3\hbar^4P_2$$
$$-8m^{*2}a_{ns}^4E_gQ_3-2m^*a_{ns}^2q^2\hbar^2E_gQ_3-11m^*a_{ns}^2q^2\hbar^2E_gR_1+4m^*a_{ns}^4E_g^2R_1-12m^*a_{ns}^2q\hbar^2E_gR_2+3q^3\hbar^4R_2), \tag{A1}$$

$$B_{ns}(\vec{q},\omega)=m^{*2}a_{ns}^2E_g^{3/2}L_1\left(\frac{2m^{*3}a_{ns}^3\omega^3}{q^5\hbar^7}-\frac{m^*a_{ns}\omega}{2q\hbar^5}+\frac{2m^{*2}a_{ns}^3E_g\omega}{q^3\hbar^7}\right)$$
$$-\frac{m^{*3}a_{ns}^4E_g^{5/2}}{4q^2\hbar^{10}}(4m^{*2}a_{ns}^4E_g^2P_3+m^*a_{ns}^2E_gq^2\hbar^2P_3+22m^*a_{ns}^2E_gq^2\hbar^2Q_1-8m^{*2}a_{ns}^4E_g^2Q_1-24m^*a_{ns}^2E_gq\hbar^2Q_2$$
$$+6q^3\hbar^4Q_2+22m^*a_{ns}^2E_gq^2\hbar^2Q_5-8m^{*2}a_{ns}^4E_g^2Q_5-6q^3\hbar^4Q_6+24m^*a_{ns}^2E_gq\hbar^2Q_6$$
$$+4m^{*2}a_{ns}^4E_g^2R_3+m^*a_{ns}^2E_gq^2\hbar^2R_3), \tag{A2}$$

$$C_{ns}(\vec{q},\omega)=\frac{m^{*3}a_{ns}^3\omega E_g^{3/2}L_2}{4q^5\hbar^7}(m^{*2}a_{ns}^2\omega^2-q^4\hbar^2+m^*a_{ns}^2q^2E_g)-\frac{m^{*3}a_{ns}^4E_g^{5/2}}{4q^2\hbar^{10}}(-11m^*a_{ns}^2E_gq^2\hbar^2P_5+4m^{*2}a_{ns}^4E_g^2P_5$$
$$+3q^3\hbar^4P_6-12m^*a_{ns}^2E_gq\hbar^2P_6-11m^*a_{ns}^2E_gq^2\hbar^2R_5+4m^{*2}a_{ns}^4E_g^2R_5-3q^3\hbar^4R_6+12m^*a_{ns}^2E_gq\hbar^2R_6), \tag{A3}$$

$$D_{ns}(\vec{q},\omega)=\frac{2m^{*7/2}a_{ns}^4\omega E_g^2L_1}{q^2\hbar^6}+\frac{m^{*7/2}a_{ns}^5E_g^3}{2q^5\hbar^{10}}(2m^*a_{ns}\omega q^4\hbar^2Q_7-6m^{*2}a_{ns}^2\omega^2q^2\hbar Q_7$$
$$+4m^{*3}a_{ns}^3\omega^3Q_7-m^*a_{ns}\omega q^4\hbar^2R_8-3m^{*2}a_{ns}^2\omega^2q^2\hbar R_8-2m^{*3}a_{ns}^3\omega^3R_8), \tag{A4}$$

$$E_{ns}(\vec{q},\omega)=-\frac{2m^{*7/2}a_{ns}^4\omega E_g^2L_1}{q^2\hbar^6}-\frac{m^{*7/2}a_{ns}^5E_g^3}{2q^5\hbar^{10}}(m^*a_{ns}\omega q^4\hbar^2P_8-3m^{*2}a_{ns}^2\omega^2q^2\hbar P_8$$
$$+2m^{*3}a_{ns}^3\omega^3P_8-2m^*a_{ns}\omega q^4\hbar^2Q_8-6m^{*2}a_{ns}^2\omega^2q^2\hbar Q_8-4m^{*3}a_{ns}^3\omega^3Q_8), \tag{A5}$$

$$F_{ns}(\vec{q},\omega)=\frac{m^{*7/2}a_{ns}^4\omega E_g^2L_2}{2q^2\hbar^6}+\frac{m^{*7/2}a_{ns}^5E_g^3}{4q^5\hbar^{10}}(m^*a_{ns}\omega q^4\hbar^2R_7-4m^{*3}a_{ns}^3\omega^3R_7), \tag{A6}$$

$$G_{ns}(\vec{q},\omega) = -\frac{m^{*7/2}a_{ns}^4\omega E_g^2 L_2}{2q^2\hbar^6} + \frac{m^{*7/2}a_{ns}^5 E_g^3}{4q^5\hbar^{10}}(m^* a_{ns}\omega q^4\hbar^2 P_7 - 4m^{*3}a_{ns}^3\omega^3 P_7), \tag{A7}$$

$$H_{ns}(\vec{q},\omega) = -\frac{m^{*7/2}a_{ns}^4\omega E_g^2 L_1}{q^2\hbar^6} - \frac{m^{*7/2}a_{ns}^5 E_g^3}{8q^2\hbar^9}(q^2\hbar^2 P_4 + 4m^* a_{ns}^2 E_g P_4 + 6q^3\hbar^2 Q_1 - 24m^* a_{ns}^2 E_g q Q_1 - 22q^2\hbar^2 Q_2$$
$$+ 8m^* a_{ns}^2 E_g Q_2 + 6q^3\hbar^2 Q_5 - 24m^* a_{ns}^2 E_g q Q_5 + 22q^2\hbar^2 Q_6 - 8m^* a_{ns}^2 E_g Q_6 - q^2\hbar^2 R_4 - 4m^* a_{ns}^2 E_g R_4), \tag{A8}$$

$$I_{ns}(\vec{q},\omega) = -\frac{m^{*7/2}a_{ns}^4\omega E_g L_2}{4q^2\hbar^6} - \frac{m^{*7/2}a_{ns}^5 E_g^3}{8q^2\hbar^9}(-3q^3\hbar^2 P_5 + 12m^* a_{ns}^2 q E_g P_5$$
$$- 11q^2\hbar^2 P_6 + 4m^* a_{ns}^2 E_g P_6 - 3q^3\hbar^2 R_5 + 12m^* a_{ns}^2 q E_g R_5 + 11q^2\hbar^2 R_6 - 4m^* a_{ns}^2 E_g R_6), \tag{A9}$$

$$J_{ns}(\vec{q},\omega) = P_1 + P_3 + P_5 + P_7 + P_8 - 2Q_1 - 2Q_3 - 2Q_5 - 2Q_7 - 2Q_8 + R_1 + R_3 + R_5 + R_7 + R_8, \tag{A10}$$

$$K_{ns}(\vec{q},\omega) = \frac{4m^* a_{ns}^2 E_g}{\hbar^2}(-P_1 - P_3 - P_5 + 2Q_1 + 2Q_3 + 2Q_5 - R_1 - R_3 - R_5)$$
$$+ \frac{4m^* a_{ns}}{\hbar}(-P_7 - 2P_8 + 2Q_7 - 2Q_8 + R_7 + 2R_8) + \frac{4m^{*2}a_{ns}^2\omega^2}{q^2\hbar^2}(P_7 + P_8 - 2Q_7 - 2Q_8 + R_7 + R_8)$$
$$+ 11q^2 P_1 - 12qP_2 + 3q^2 P_3 - 4qP_4 + 3q^2 P_5 + 4qP_6 + 3q^2 P_7 + 6q^2 P_8$$
$$- 6q^2 Q_1 + 16qQ_2 + 2q^2 Q_3 - 6q^2 Q_5 - 16qQ_6 + 11q^2 R_1 + 12qR_2 + 3q^2 R_3 + 4qR_4 + 3q^2 R_5 - 4qR_6$$
$$+ 3q^2 R_7 + 6q^2 R_8, \tag{A11}$$

where

$$L_1 = \left[\left(\frac{q^2}{4} + \frac{m^{*2}a_{ns}^2\omega^2}{q^2\hbar^2} + \frac{m^* a_{ns}^2 E_g}{\hbar^2}\right)^2 - \frac{m^{*2}a_{ns}^2\omega^2}{\hbar^2}\right]^{-1} \tag{A12}$$

and

$$L_2 = \left[\left(q^2 + \frac{m^{*2}a_{ns}^2\omega^2}{q^2\hbar^2} + \frac{m^* a_{ns}^2 E_g}{\hbar^2}\right)^2 - \frac{4m^{*2}a_{ns}^2\omega^2}{\hbar^2}\right]^{-1}. \tag{A13}$$

The parameters P_i, Q_i, and R_i, $i = 1, 2, 3, \ldots, 8$, are the solutions of the equations

$$X_1 + X_3 + X_5 + X_7 + X_8 = 0, \tag{A14}$$

$$-2qX_1 + X_2 - qX_3 + X_4 + X_6 - (b+2q)X_7 - (c+2q)X_8 = 0, \tag{A15}$$

$$(bc - 6bq - 6cq)X_1 + (b + c - 6q)X_2 + (bc - 5bq - 5cq - 5q^2)X_3 + (b + c - 4q)X_4$$
$$+ (bc - 4bq - 4cq - 8q^2)X_5 + (b + c - 2q)X_6 + (a - 6cq)X_7 + (a - 6bq)X_8 = 0, \tag{A16}$$

$$[-6bcq + (b+c)(13q^2 + 2a) - 6q(2q^2 + a)]X_1 + (bc - 6bq - 6cq + 13q^2 + 2a)X_2$$
$$+ [-5bcq + 2(b+c)(4q^2 + a) - 2q(2q^2 + 3a)]X_3 + [bc - 4q(b+c) + 4q^2 + 2a]X_4$$
$$+ [-4bcq + (b+c)(5q^2 + 2a) - 2q(q^2 + 3a)]X_5 + [bc - 2q(b+c) + q^2 + 2a]X_6$$
$$+ [-12q(q^2 + a) + c(3a + 13q^2)]X_7 + [-12q(q^2 + a) + b(3a + 13q^2)]X_8 = 0, \tag{A17}$$

$$[bc(2a + 13q^2) - 6q(2q^2 + a)(b + c) + (q^2 + a)(4q^2 + a)]X_1 + [-6bcq + (b+c)(2a + 13q^2) - 6q(2q^2 + a)]X_2$$

$$+[2bc(4q^2+a)-2q(2q^2+3a)(b+c)+a(8q^2+a)]X_3+[-4bcq+2(2q^2+a)(b+c)-4qa]X_4$$

$$+[bc(5q^2+2a)-2q(q^2+3a)(b+c)+a(5q^2+a)]X_5+[-2bcq+(q^2+2a)(b+c)-2aq]X_6$$

$$+[4q^4+18aq^2+3a^2-12cq(q^2+a)]X_7+[4q^4+18aq^2+3a^2-12bq(q^2+a)]X_8=0\,, \tag{A18}$$

$$[(b+c)(q^2+a)(4q^2+a)-6bcq(2q^2+a)]X_1+[bc(13q^2+2a)-6q(2q^2+a)(b+c)+(q^2+a)(4q^2+a)]X_2$$

$$+[-2bcq(2q^2+3a)+a(b+c)(8q^2+a)-aq(4q^2+a)]X_3+[2bc(2q^2+a)-4q\,a(b+c)+a(4q^2+a)]X_4$$

$$+[-2bcq(q^2+3a)+a(b+c)(5q^2+a)-2aq(q^2+a)]X_5+[bc(q^2+2a)-2qa(b+c)+a(q^2+a)]X_6$$

$$+[-6aq(2q^2+a)+c(4q^4+18q^2a+3a^2)]X_7+[-6aq(2q^2+a)+b(4q^4+18q^2a+3a^2)]X_8=0\,, \tag{A19}$$

$$bc(q^2+a)(4q^2+a)X_1+[(b+c)(q^2+a)(4q^2+a)-6bcq(2q^2+a)]X_2$$

$$+[abc(8q^2+a)-aq(b+c)(4q^2+a)]X_3+[-4abcq+a(b+c)(4q^2+a)]X_4$$

$$+[abc(5q^2+a)-2aq(b+c)(q^2+a)]X_5+[-2abcq+a(b+c)(q^2+a)]X_6$$

$$+[a(q^2+a)(4q^2+a)-6acq(2q^2+a)]X_7+[a(q^2+a)(4q^2+a)-6abq(2q^2+a)]X_8=0\,, \tag{A20}$$

$$bc(q^2+a)(4q^2+a)X_2-abcq(4q^2+a)X_3+abc(4q^2+a)X_4-2abcq(q^2+a)X_5$$

$$+abc(q^2+a)X_6+ac(q^2+a)(4q^2+a)X_7+ab(q^2+a)(4q^2+a)X_8=1\,. \tag{A21}$$

The solution in Eqs. (A14)–(A21) is $X_i=P_i$, $i=1, 2, 3, \ldots, 8$ with $a=(m^*\alpha_{ns}^2E_g/\hbar^2)$, $b=-q-(m^*a_{ns}\omega/q\hbar)$, and $c=-\frac{1}{2}q-(m^*a_{ns}\omega/q\hbar)$; $X_i=Q_i$, $i=1, 2, 3, \ldots, 8$, with $a=(m^*\alpha_{ns}^2E_g/\hbar^2)$, $b=-\frac{1}{2}q-(m^*a_{ns}\omega/q\hbar)$, and $c=-(3q/2)-(m^*a_{ns}\omega/q\hbar)$; $X_i=R_i$, $i=1, 2, 3, \ldots, 8$, with $a=(m^*\alpha_{ns}^2E_g/\hbar^2)$, $b=q-(m^*a_{ns}\omega/q\hbar)$, $c=(q/2)-(m^*a_{ns}\omega/q\hbar)$, and q being changed to $-q$ in Eqs. (A14)–(A21).

---

*Partially supported by National Science Council of the Republic of China.

[1]P. A. Wolff, Phys. Rev. 171, 436 (1968).

[2]K. C. Rustagi, C. S. Warke, and S. S. Jha, Nuovo Cimento B 58, 93 (1968).

[3]R. W. Bierig, M. H. Weiler, and B. Lax, Phys. Rev. 186, 747 (1969).

[4]C. C. Wang and N. W. Ressler, Phys. Rev. 188, 291 (1969).

[5]Chhi-Chong Wu and H. N. Spector, Phys. Rev. B 3, 3979 (1971).

[6]Chhi-Chong Wu and J. Tsai, Phys. Rev. B 5, 4008 (1972).

[7]S. Sharma and U. P. Phadke, Phys. Rev. Lett. 29, 272 (1972).

[8]G. E. Smith, G. A. Baraff, and J. M. Rowell, Phys. Rev. 135, A1118 (1964).

[9]Yu. M. Gal'perim, Fiz. Tverd. Tela 10, 2338 (1968) [Sov. Phys.–Solid State 10, 1840 (1969)].

[10]M. Giura, R. Marcon, T. Papa, and F. Wanderlingh, Nuovo Cimento B 63, 192 (1969).

[11]V. Ya. Demikhovskii and A. P. Kopasov, Fiz. Tverd. Tela 13, 2468 (1971) [Sov. Phys.–Solid State 13, 2068 (1972)].

[12]J. F. Koch and J. D. Jensen, Phys. Rev. 184, 643 (1969).

[13]R. J. Dinger and A. W. Lawson, Phys. Rev. B 1, 2418 (1970); Phys. Rev. B 3, 253 (1971); Phys. Rev. B 7, 5215 (1973).

[14]M. H. Cohen, Phys. Rev. 121, 387 (1961).

[15]H. N. Spector, 1968 Sendai Symposium on Acousto-electronics, Sendai, Japan, 1968, p. 47 (unpublished).

[16]Chhi-Chong Wu and H. N. Spector, J. Appl. Phys. 43, 2937 (1972).

[17]G. A. Antcliffe and R. T. Bate, Phys. Rev. 160, 531 (1967).

[18]M. H. Cohen and E. I. Blount, Philos. Mag. 5, 115 (1960).

[19]G. A. Baraff, Phys. Rev. 137, A842 (1965).

[20]L. A. Fal'kovskii, Usp. Fiz. Nauk 94, 3 (1968) [Sov. Phys.–Usp. 11, 1 (1969)].

[21]H. N. Spector, in *Solid State Physics*, edited by F. Seitz and D. Turnbull (Academic, New York, 1966), Vol. 19, p. 291.

[22]M. J. Harrison, Phys. Rev. 119, 1260 (1960).

[23]Chhi-Chong Wu, J. Tsai, and H. N. Spector, Phys. Rev. B 7, 3836 (1973).

[24]V. L. Gurevich, V. G. Skobov, and Yu. A. Firsov, Zh. Eksp. Teor. Fiz. 40, 786 (1961) [Sov. Phys.–JETP 13, 552 (1961)].

[25]S. H. Liu and A. M. Toxen, Phys. Rev. 138, A487 (1965).

[26]F. G. Bass and I. B. Levinson, Zh. Eksp. Teor. Fiz. 49, 914 (1965) [Sov. Phys.–JETP 22, 635 (1966)].

[27]Chhi-Chong Wu and J. Tsai, Appl. Phys. Lett. 22, 297 (1973).

[28]R. K. Bakanas, Fiz. Tverd. Tela 12, 3408 (1970) [Sov. Phys.–Solid State 12, 2769 (1971)].